Table 2 – Thickness of granulation tissue and cell types in the granulation tissue

Materials	Granulation tissue thickness (μm)	Cells inducted by materials in granulation tissue
de-F-MWCNT blocks	40–70	Lymphocyte Cells with large cytoplasmic spaces like fibroblasts Fibroblast Foreign body giant cell
MWCNT/resin blocks	290–340	Lymphocyte Cells with large cytoplasmic spaces like fibroblasts Blood capillary Macrophage
PMMA	40–120	Macrophage Eosinophil Fibroblast Blood capillary Foreign body giant cell
Ni	300–1000	Necrotic cell Macrophage Neutrophil Blood capillary Red blood cell

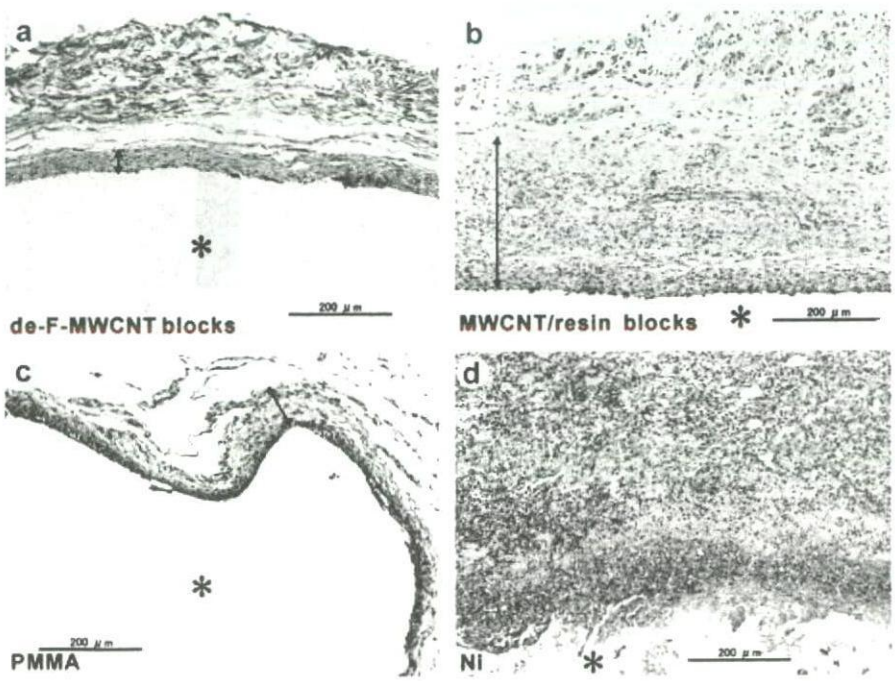

Fig. 3 – Typical low-magnification optical photographs of soft tissue response to (a) de-F-MWCNT blocks, (b) MWCNT/resin blocks, (c) PMMA, and (d) pure Ni metal at 1 week after surgery. Samples were stained with hematoxylin and eosin. Asterisk (•) is the place where samples were implanted. Arrow span shows granulation tissue thickness. In the case of pure Ni metal, necrosed tissue was observed.

tive tissue at the early implantation stage. However, as hydroxyapatite cement [35] or hydroxyapatite [36] synthesized by spark plasma sintering method show the same tissue response as that elicited with the use of de-F-MWCNT blocks, the latter seem to possess sufficient biocompatibility.

The in vivo tissue response to pure MWCNTs [37,38], MWCNTs with carboxyl groups [39] and hat-stacked carbon nanofibers [40] as determined from histological and high-resolution transmission electron microscope (HRTEM) observations suggest the absence of an acute inflammatory response. Although in vivo tests using CN_x nanotubes [41,42], in vitro and in vivo tests of various functionalized CNTs [43,44] and carbon nanohorn [45] have shown these materials to be biocompatible, use of MWCNT/resin blocks

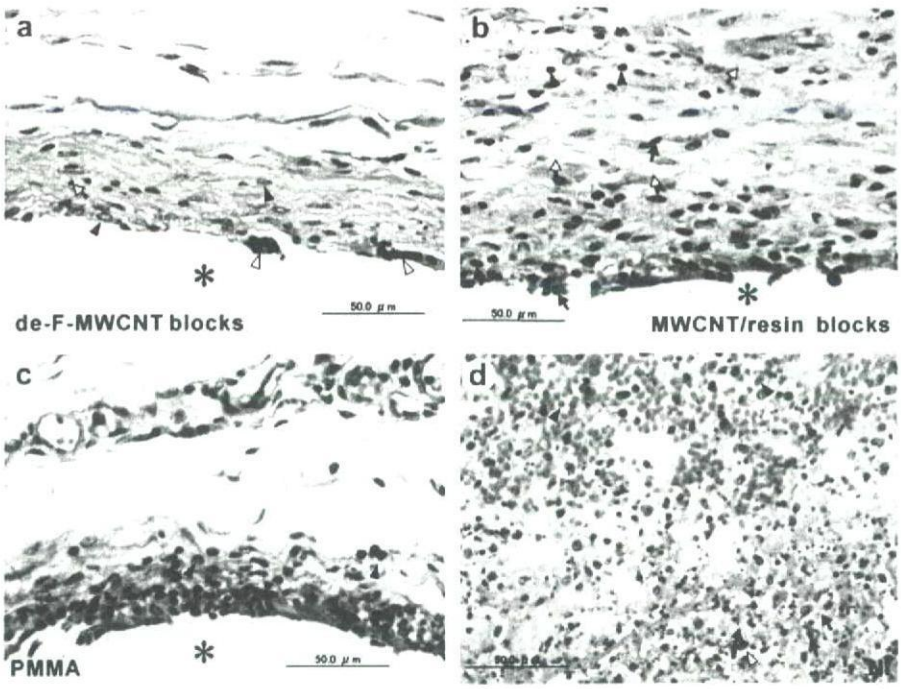

Fig. 4 – Typical high-magnification optical photographs of soft tissue response to (a) de-F-MWCNT blocks, (b) MWCNT/resin blocks, (c) PMMA, and (d) pure Ni metal at 1 week after surgery. Samples were stained with hematoxylin and eosin. Asterisk (*) is the place where samples were implanted. (a) A few lymphocytes (white arrow), immature fibroblasts (arrow head), and foreign-body giant cells (white arrow head) are seen in the granulation tissue, which is indicative of a slight inflammatory response. (b) Many lymphocytes (arrow head), cell with large cytoplasmic spaces like fibroblasts, macrophages (arrow), and the dilatation of blood capillaries (white arrow) are observed. (c) Immature fibroblasts, macrophages, eosinophils (arrow head), and the dilatation of blood capillary can be seen. (d) Many macrophages and neutrophils (white arrow head), necrosed tissue (arrow; no nuclei, light pink color) and red blood cells (arrow head) external to the necrosed tissue appear. The inflammatory response to pure Ni metal is very strong.

elicits an inflammatory response. Aircraft production workers exposed to resin containing C/C have developed dermatitis [46]. In our case, although there is no amorphous carbon in the purified MWCNTs, amorphous carbon is present in the MWCNT/resin blocks as determined by HRTEM observations (Figs. S1 and S2), which indicates that phenol resins were carbonized. The presence of functional groups on the de-F-MWCNT blocks and MWCNT/resin blocks was established by FT-IR spectroscopy using a transmission method (KBr pellet). The FT-IR spectrum of carbon nanotubes with a higher defect concentration is characterized by the presence of a broader band at 1220 cm^{-1} that is assigned to a signal derived from the carbon skeleton [47,48], and the band present at 1584 cm^{-1} in the two spectra is associated with the stretching vibration of the aromatic C=C group (Fig. S3). The band assigned to the C–F covalent bond is absent in the FT-IR spectrum of the de-F-MWCNT blocks, while a broader band located at 1203 cm^{-1} and assigned to the carbon skeleton is present [27]. On the other hand, in the MWCNT/resin blocks, the slight bands at 2844 and 2921 cm^{-1} assigned to the stretching vibration of the C–H group are present (Fig. S3). However, the presence of the phenol is not reliable because of poor IR absorption. Recently, Lison and Fubini groups [49,50] have investigated the effect of the presence of CNT framework and surface defects on lung toxicity of MWCNTs. They explored the physicochemical determinants of these toxic responses with progressively and selectively modified CNTs (i) by grinding (introducing structural defects) and heating either in a vacuum at 873 K (causing reduction of oxygenated carbon functionalities and reduction of oxidized metals) or in an inert atmosphere at 2673 K (causing elimination of metals and annealing of defects) and (ii) by heating at 2673 K in an inert atmosphere and grinding the thermally treated MWCNTs (introducing defects in a metal-deprived carbon framework). In vivo and vitro experiments performed to evaluate lung response in bronchoalveolar lavage fluid (lactase dehydrogenase (LDH), proteins, cellar infiltration, interleukin-1 beta (IL-1β), and tumor necrosis factor-alpha (TNF-α)) using Wistar rats and to assess the genotoxic potential of the modified CNTs cytokinesis block micronucleus assay, respectively. From the physicochemical aspects, the potential of the modified CNT to scavenge hydroxyl radicals was evaluated by means of electron spin resonance spectroscopy. The results show that acute pulmonary toxicity and the genotoxicity of CNT were reduced upon heating but restored upon grinding. In addition, the original ground MWCNTs exhibited a scavenging activity toward hydroxyl radicals, which was eliminated by heating at 2673 K but restored upon grinding. This scavenging activity, related to the presence of defects, appears to go paired with the genotoxic and inflammatory

potential of MWCNT. They conclude that the intrinsic toxicity of CNT is mainly mediated by the presence of defective sites in their carbon framework. From the point of view of the presence of defective carbon materials, in the MWCNT/resin blocks, the inflammation response might be accounted for by the presence of amorphous carbon-like unidentified carbon frameworks that remain due to imperfect carbonization of the resin.

4. Conclusion

We found that the binder-free MWCNT blocks cross-linked by de-fluorination possess biocompatibility as assessed following the in vivo implantation of rats. As this block is light, strong, and biocompatible, it can be applied to internal bone plates [51] or bone. In the latter application, a critical issue concerning the use of carbon composite materials as an alternative hard tissue material has to do with the lack of strongly adhering tissue to the carbon materials. However, it is hoped that the use of CNTs can obviate this problem. For example, we found that osteoblasts tightly adhered to a scaffold comprising CNT [15,17]. Additionally, CNTs are able to bind [52], immobilize [53,54], and trap proteins [24,25], and hydroxyapatite separates out on the surface of CNTs [18,38,55,56]. If three-dimensional highly porous carbon nanotube blocks in which cells could live could be prepared by the method for producing active cross-linking sites on nanotube surfaces via de-fluorination of multi-walled carbon nanotubes, carbon nanotube biomaterials onto which tissue can tightly adhere might be designed using a combination of protein, hydroxyapatite and CNTs.

Acknowledgments

This work was supported by a Grant-in-Aid for Young Research (A) 19686038, and Exploratory Research 19656175 from the Ministry of Education, Science, Culture and Sport of Japan, and Health and Labor Sciences Research Grant No. H18-chemistry-006 from the Ministry of Health, Labor and Welfare.

Appendix A. Supplementary material

TEM image of MWCNT/resin blocks (Fig. S1), elemental analysis of amorphous carbon of MWCNT/resin blocks by TEM-EDX (Fig. S2), and functional group analysis of de-F-MWCNT and MWCNT/resin blocks by FT-IR (Fig. S3).

Supplementary data associated with this article can be found, in the online version, at doi:10.1016/j.carbon.2008.08.003.

REFERENCES

[1] Gott VL, Whiffen JD, Dutton RC. Heparin bonding on colloidal graphite surfaces. Science 1963;142:1297–8.
[2] Bokros JC. Carbon biomedical devices. Carbon 1977;15:355–71.
[3] Hulbert SF, Bokros JC. Use of carbons in dental and orthopedic implants. Carbon 1977;15:429.
[4] Makisalo S, Paavolainen P, Gronblad M, Holmstrom T. Tissue reactions around two alloplastic ligament substitute materials: experimental study on rats with carbon fibres and polypropylene. Biomaterials 1989;10:105–8.
[5] Demmer P, Fowler M, Marino AA. Use of carbon-fibers in the reconstruction of knee ligaments. Clin Orthop Relat Res 1991;271:225–32.
[6] Brüchmann H, Huttinger KJ. Carbon, a promising material in endoprosthetics. Part 1: the carbon materials and their mechanical properties. Biomaterials 1980;1:67–72.
[7] Howling GI, Sakoda H, Antonarulrajah A, Marrs H, Stewart TD, Appleyard S, et al. Biological response to wear debris generated in carbon based composites as potential bearing surfaces for artificial hip joints. J Biomed Mater Res B 2003;67:758–64.
[8] Howling GI, Ingham E, Sakoda H, Stewart TD, Fisher J, Antonarulrajah A, et al. Carbon–carbon composite bearing materials in hip arthroplasty: analysis of wear and biological response to wear debris. J Mater Sci Mater Med 2004;15:91–8.
[9] Jenkins GM, de Carvalho FX. Biomedical applications of carbon fibre reinforced carbon in implanted prostheses. Carbon 1977;15:33–7.
[10] Slivka MA, Chu CC, Adisaputro IA. Fiber–matrix interface studies on bioabsorbable composite materials for internal fixation of bone fractures. 1. Raw material evaluation and measurement of fiber–matrix interfacial adhesion. J Biomed Mater Res 1997;36:469–77.
[11] Pantarotto D, Singh R, McCarthy D, Erhardt M, Briand JP, Prato M, et al. Functionalized carbon nanotubes for plasmid DNA gene delivery. Angew Chem Int Ed 2004;43:5242–6.
[12] Kam NWS, Liu Z, Dai H. Carbon nanotubes as intracellular transporters for proteins and DNA: an investigation of the uptake mechanism and pathway. Angew Chem Int Ed 2004;45:577–81.
[13] Lu Q, Moore JM, Huang G, Mount AS, Rao AM, Larcom LL, et al. RNA polymer translocation with single-walled carbon nanotubes. Nano Lett 2004;4:2473–7.
[14] Correa-Duarte MA, Wagner N, Rojas-Chapana J, Morsczeck C, Thie M, Giersig M. Fabrication and biocompatibility of carbon nanotube-based 3D networks as scaffolds for cell seeding and growth. Nano Lett 2004;4:2233–6.
[15] Aoki N, Yokoyama A, Nodasaka Y, Akasaka T, Uo M, Sato Y, et al. Cell culture on a carbon nanotube scaffold. J Biomed Nanotechnol 2005;1:402–5.
[16] Lovat V, Pantarotto D, Lagostena L, Cacciari B, Grandolfo M, Righi M, et al. Carbon nanotube substrates boost neuronal electrical signaling. Nano Lett 2005;5:1107–10.
[17] Aoki N, Yokoyama A, Nodasaka Y, Akasaka T, Uo M, Sato Y, et al. Strikingly extended morphology of cells grown on carbon nanotubes. Chem Lett 2006;35:508–9.
[18] Zanello LP, Zhao B, Hu H, Haddon RC. Bone cell proliferation on carbon nanotubes. Nano Lett 2006;6:562–7.
[19] Endo M, Koyama S, Matsuda Y, Hayashi T, Kim YA. Thrombogenicity and blood coagulation of a microcatheter prepared from carbon nanotube-nylon-based composite. Nano Lett 2005;5:101–5.
[20] Koyama S, Haniu H, Osaka K, Koyama H, Kuroiwa N, Endo M, et al. Medical application of carbon-nanotube-filled nanocomposites: the microcatheter. Small 2006;2:1406–11.
[21] Wang W, Watari F, Omori M, Liao S, Zhu YH, Yokoyama A, et al. Mechanical properties and biological behavior of carbon nanotube/polycarbosilane composites for implant materials. J Biomed Mater Res B 2007;82:223–30.
[22] Wang W, Omori M, Watari F, Yokoyama A. Novel bulk carbon nanotube materials for implant by spark plasma sintering. Dent Mater J 2004;24:478–86.

[23] Yu MF, Lourie O, Dyer MJ, Moloni K, Kelly TF, Ruoff RS. Strength and breaking mechanism of multiwalled carbon nanotubes under tensile load. Science 2000;287:637–40.
[24] Lin Y, Allard LF, Sun YP. Protein-affinity of single-walled carbon nanotubes in water. J Phys Chem B 2004;108: 3760–4.
[25] Salvador-Morales C, Flahaut E, Sim E, Sloan J, Green MLH, Sim RB. Complement activation and protein adsorption by carbon nanotubes. Mol Immunol 2006;43:193–201.
[26] Romo-Herrera JM, Terrones M, Terrones H, Dag S, Meunier V. Covalent 2D and 3D networks from 1D nanostructures: designing new materials. Nano Lett 2007;7:570–6.
[27] Sato Y, Ootsubo M, Yamamoto G, Van Lier G, Terrones M, Hashiguchi S, et al. Super-robust, lightweight, conducting carbon nanotube blocks cross-linked by de-fluorination. ACS Nano 2008;2:348–56.
[28] Shankar R, Greisler HP. In: Greco RS, editor. Implantation biology: the host response and biomedical devices. Boca Raton: CRC Press; 1994. p. 67–80.
[29] Tamura K, Takashi N, Kumazawa R, Watari F, Totsuka Y. Effects of particle size on cell function and morphology in titanium and nickel. Mater Trans 2002;43:3052–7.
[30] Oberdörster G, Stone V, Donaldson K. Toxicology of nanoparticles: a historical perspective. Nanotoxicology 2007;1:2–25.
[31] Lewinski N, Colvin V, Drezek R. Cytotoxicity of nanoparticles. Small 2008;4:26–49.
[32] Uo M, Watari F, Yokoyama A, Matsuno H, Kawasaki T. Tissue reaction around metal implants observed by X-ray scanning analytical microscopy. Biomaterials 2001;22:677–85.
[33] Matsuno H, Yokoyama A, Watari F, Uo M, Kawasaki T. Biocompatibility and osteogenesis of refractory metal implants, titanium, hafnium, niobium, tantalum and rhenium. Biomaterials 2001;22:1253–62.
[34] MacNeill SR, Cobb CM, Rapley JW, Glaros AG, Spencer P. In vivo comparison of synthetic osseous graft materials – a preliminary study. J Clin Periodontol 1999;26:239–45.
[35] Yokoyama A, Matsuno H, Yamamoto S, Kawasaki T, Kohgo T, Uo M, et al. Tissue response to a newly developed calcium phosphate cement containing succinic acid and carboxymethyl-chitin. J Biomed Mater Res A 2003;64:491–501.
[36] Gu YW, Khor KA, Cheang P. Bone-like apatite layer formation on hydroxyapatite prepared by spark plasma sintering (SPS). Biomaterials 2005;25:4127–34.
[37] Koyama S, Endo M, Kim YA, Hayashi T, Yanagisawa T, Osaka K, et al. Role of systemic T-cells and histopathological aspects after subcutaneous implantation of various carbon nanotubes in mice. Carbon 2006;44:1079–92.
[38] Usui Y, Aoki K, Narita N, Murakami N, Nakamura I, Nakamura K, et al. Carbon nanotubes with high bone-tissue compatibility and bone-formation acceleration effects. Small 2008;4:240–6.
[39] Sato Y, Yokoyama A, Shibata KI, Akimoto Y, Ogino S, Nodasaka Y, et al. Influence of length on cytotoxicity of multi-walled carbon nanotubes against human acute monocytic leukemia cell line THP-1 *in vitro* and subcutaneous tissue of rats *in vivo*. Mol BioSyst 2005;1:176–82.
[40] Yokoyama A, Sato Y, Nodasaka Y, Yamamoto S, Kawasaki T, Shindoh M, et al. Biological behavior of hat-stacked carbon nanofibers in the subcutaneous tissue in rats. Nano Lett 2005;5:157–61.
[41] Carrero-Sanchez JC, Elias AL, Mancilla R, Arrellin G, Terrones H, Laclette JP, et al. Biocompatibility and toxicological studies of carbon nanotubes doped with nitrogen. Nano Lett 2006;6:1609–16.
[42] Elías AL, Carrero-Sánchez JC, Terrones H, Endo M, Laclette JP, Terrones M. Viability studies of pure carbon- and nitrogen-doped nanotubes with entamoeba histolytica: from amoebicidal to biocompatible structures. Small 2007;3:1723–9.
[43] Kostarelos K, Lacerda L, Pastorin G, Wu W, Wieckowski S, Luangsivilay J, et al. Cellular uptake of functionalized carbon nanotubes is independent of functional group and cell type. Nat Nanotechnol 2007;2:108–13.
[44] Dumortier H, Lacotte S, Pastorin G, Marega R, Wu W, Bonifazi D, et al. Functionalized carbon nanotubes are non-cytotoxic and preserve the functionality of primary immune cells. Nano Lett 2006;6:1522–8.
[45] Miyawaki J, Yudasaka M, Azami T, Kubo Y, Iijima S. Toxicity of single-walled carbon nanohorns. ACS Nano 2008;2:213–26.
[46] Eedy DJ. Carbon-fibre-induced airborne irritant contact dermatitis. Contact Dermatitis 1996;35:362–3.
[47] Shaffer MSP, Fan X, Windle AH. Dispersion and packing of carbon nanotubes. Carbon 1998;36:1603–12.
[48] Ogino S, Sato Y, Yamamoto G, Sasamori K, Kimura H, Hashida T, et al. Relation of the number of cross-links and mechanical properties of multi-walled carbon nanotube films formed by a dehydration condensation reaction. J Phys Chem B 2006;110:23159–63.
[49] Muller J, Huaux F, Fonseca A, Nagy JB, Moreau N, Delos M, et al. Structural defects play a major role in the acute lung toxicity of multiwall carbon nanotubes: toxicological aspects. Chem Res Toxicol 2008. doi:10.1021/tx800101p.
[50] Fenoglio I, Greco G, Tomatis M, Muller J, Raymundo-Pinero E, Beguin F, et al. Structural defects play a major role in the acute lung toxicity of multiwall carbon nanotubes: physicochemical aspects. Chem Res Toxicol 2008. doi:10.1021/tx800100s.
[51] Fitzer E, Heüttiner W, Claes L, Kinzl L. Torsional strength of carbon fibre reinforced composites for the application as internal bone plates. Carbon 1980;18:383–7.
[52] Baker SE, Cai W, Lasseter TL, Weidkamp KP, Hamers RJ. Covalently bonded adducts of deoxyribonucleic acid (DNA) oligonucleotides with single-wall carbon nanotubes: synthesis and hybridization. Nano Lett 2002;2:1413–7.
[53] Balavoine F, Schultz P, Richard C, Mallouh V, Ebbesen TW, Mioskowski C. Helical crystallization of proteins on carbon nanotubes: a first step towards the development of new biosensors. Angew Chem Int Ed 1999;38:1912–5.
[54] Chen RJ, Zhang Y, Wang D, Dai H. Noncovalent sidewall functionalization of single-walled carbon nanotubes for protein immobilization. J Am Chem Soc 2001;123:3838–9.
[55] Akasaka T, Watari F, Sato Y, Tohji K. Apatite formation on carbon nanotubes. Mater Sci Eng C 2006;26:675–8.
[56] Zhao B, Hu H, Mandal SK, Haddon RC. A bone mimic based on the self-assembly of hydroxyapatite on chemically functionalized single-walled carbon nanotubes. Chem Mater 2005;17:3235–41.

カーボンナノチューブの細胞内挙動

横山敦郎*

JJSB

Biological behavior of carbon nanotubes

The tissue response to multi wall carbon nanotubes (MWCNTs) and hat-stacked carbon nanofibers (H-CNFs) were investigated to evaluate biocompatibility of carbon nanosubstances. MWCNTs and H-CNFs were implanted in the subcutaneous tissue of rats. Histological and ultrastructural observations revealed that MWCNTs and H-CNFs were not acutely toxic in the subcutaneous tissue and englobed by phagocytes. Possibility of structural changes of H-CNF was shown, while those of MWCNTs was not. It was suggested that the size and structure of carbon nanosubstances influenced their biological behavior.

カーボンナノ物質に対する生体反応を明らかにするため，ハット積層型カーボンナノファイバー(H-CNFs)と多層カーボンナノチューブ(MWCNTs)をラット皮下組織に埋入し，組織学的，超微細構造学的に検索した．両者ともに，急性毒性は認められず，マクロファージにより貪食されることが示された．MWCNTsの構造には変化が認められなかったが，H-CNFsでは，短縮や構造の変化が生じている可能性が示され，ナノ物質のサイズや構造は，細胞内挙動に影響を与えることが示唆された．

*Atsuro Yokoyama**

Key words：多層カーボンナノチューブ(multi wall carbon nanotubes)，ハット積層型カーボンナノファイバー(hat-stacked carbon nanofibers)，生物学的挙動，超微細構造学的検索

1991年，Iijimaによって発見されたカーボンナノチューブ[1]は，その特徴的な電気的，物理的，および化学的性質から，工業界において注目を集め多くの基礎研究がなされている．生体材料としても，カーボンナノ物質の一種であるフラーレンやナノホーンは，DDSや遺伝子導入の際の担体として研究が進められている[2,3]．

筆者らも，カーボンナノ物質を生体材料として再生医療に応用すること，特に細胞培養用スカフォールドの開発を目的に研究を進めている[4~6]．生体材料にとって，安全性はいうまでもなく最も重要な所要性質であるが，ナノ物質の医学領域への応用に際して，ナノ物質の毒性やこれらの物質に対する生体の反応についての研究は少ないため不明な点が多く，ナノ物質に対する安全性はいまだ確立されているとはいいがたい．細胞毒性をはじめとする*in vitro*での報告がなされるようになり[7~9]，*in vivo*における生体反応も最近ようやく報告されるようになってきた[10~14](カーボンナノチューブに関しての毒性評価の詳細については，本号の田路・佐藤論文を参照されたい)．中皮腫などのアスベスト被曝長期後の病変が最近大きな社会問題になっていることからも，*in vivo*での研究は必須であると考えられる．このような状況から，筆者らは，再生医療への応用とともに，カーボンナノ物質に対する生体反応についての研究を行っている[15~19]．

本稿においては，皮下組織におけるカーボンナノ物質に対する反応，特に，カーボンナノ物質のサイズ(大きさ)と構造の違いによる細胞内挙動について述べたい．

筆者らが研究をはじめた当初は，カーボンナノチューブやフラーレンについて精製された状態での入手が困難であったこともあり，共同研究を行っている東北大学大学院環境科学研究科の田路研究室よ

* Department of Oral Functional Prosthodontics, Division of Oral Functional Science, Graduate School of Dental Medicine, Hokkaido University　北海道大学大学院歯学研究科口腔機能学講座口腔機能補綴学教室

[略歴]　1984年 北海道大学歯学部卒業．1988年 同 大学大学院歯学研究科修了(歯学博士)，同 大学歯学部助手．2002年 同 大学歯学部附属病院講師．2005年 同 大学大学院歯学研究科教授，現在に至る．専門：歯科補綴学，骨補填材，デンタルインプラントなどの生体材料に対する*in vivo*の反応，ナノ物質の生体材料への応用．趣味：読書

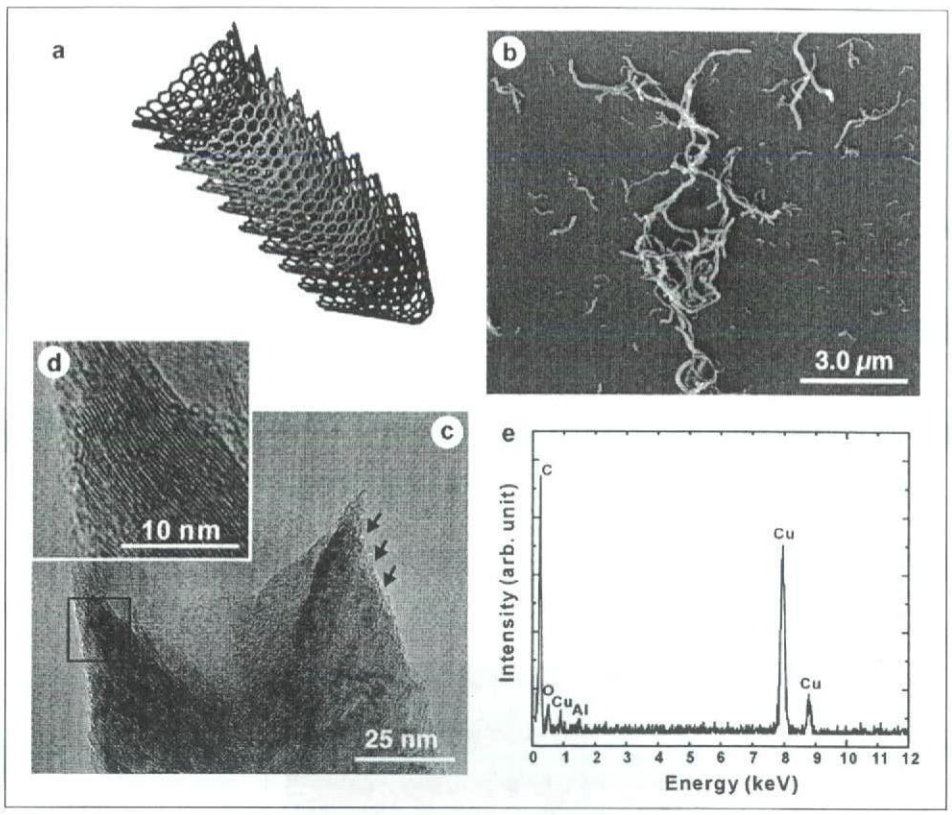

図1　ハット積層型カーボンナノファイバー(H-CNFs)(Yokoyama A et al., 2005[15]より一部改変)
a：H-CNFs模式図．b：SEM像．c：TEM像．矢印：グラフェンエッヂ．d：cの拡大像．e：EDX分析

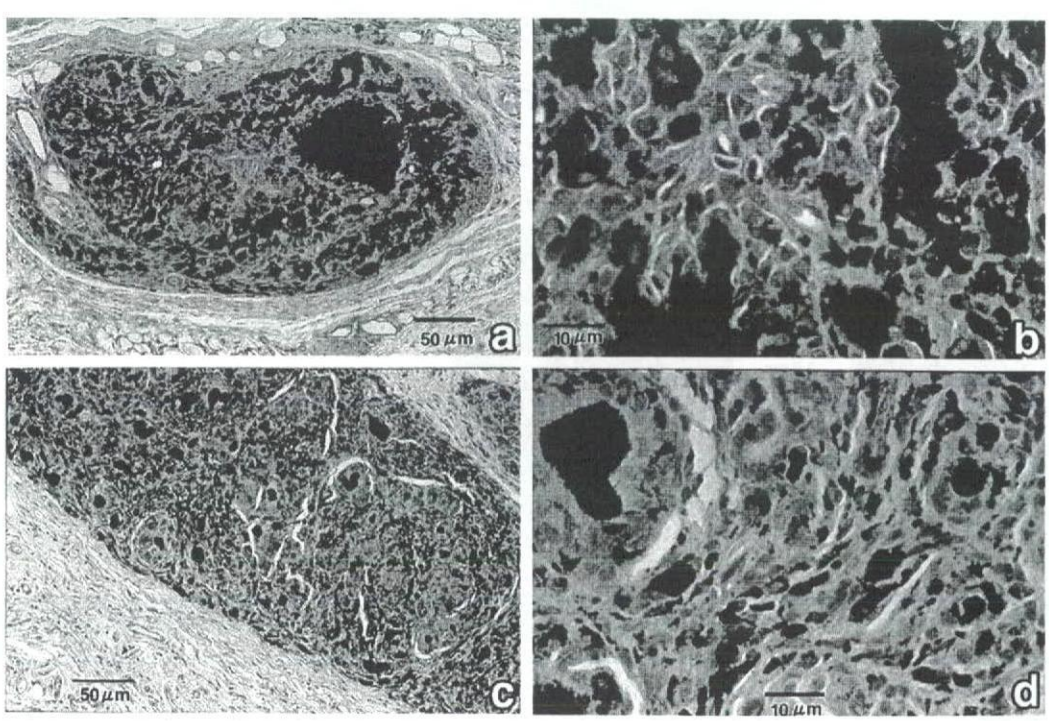

図2　H-CNFs皮下埋入後の組織像(Yokoyama A et al., 2005)[15]
a：埋入1週後．b：aの拡大像．c：埋入4週後．d：cの拡大像

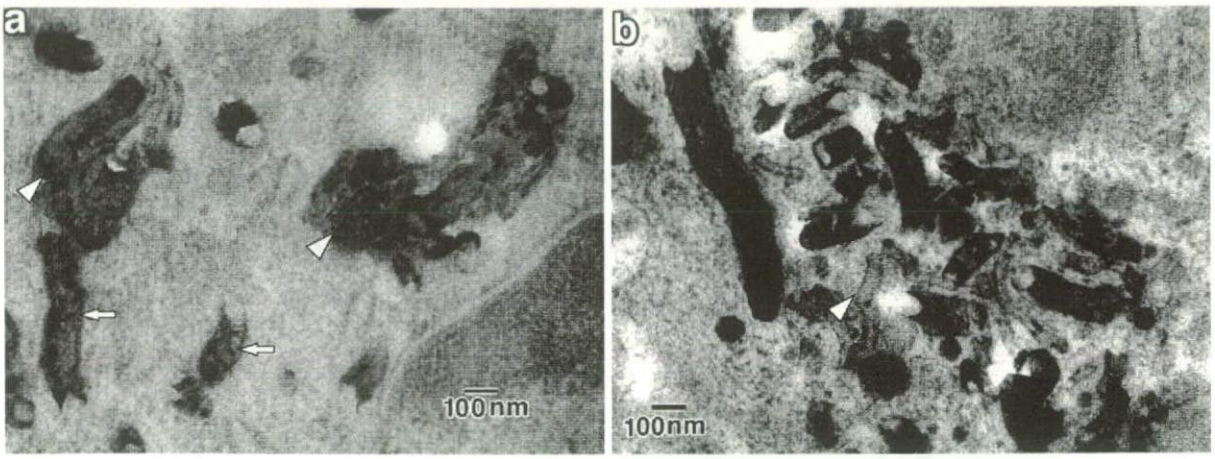

図3　H-CNFs 皮下埋入後の TEM 像
（Yokoyama A et al., 2005）[15]
a：埋入 1 週後．矢印：H-CNFs．矢頭：凝集した H-CNFs
b：埋入 4 週後．矢頭：半透明化した H-CNFs

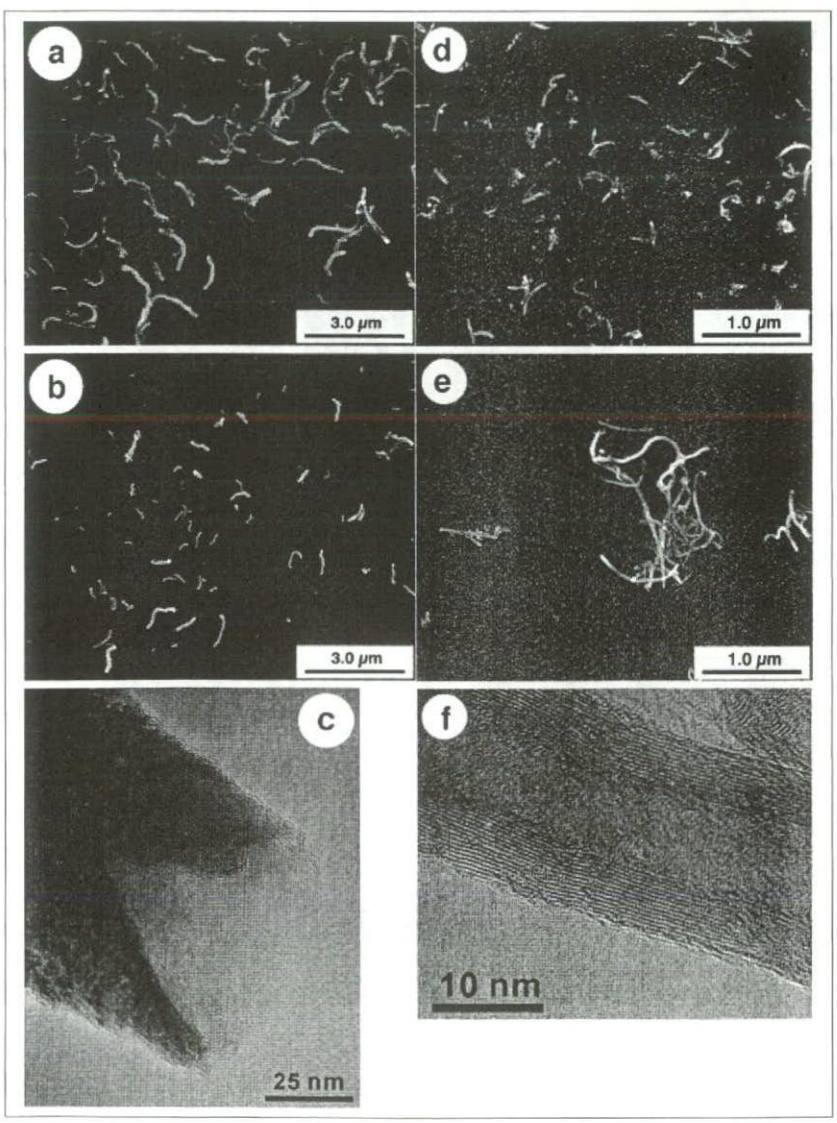

図4
サイズを制御した H-CNFs と MWCNTs
a：1200H-CNFs SEM 像
b：600H-CNFs SEM 像
c：H-CNFs TEM 像
d：220MWCNTs SEM 像
e：825MWCNTs SEM 像
f：MWCNTs TEM 像

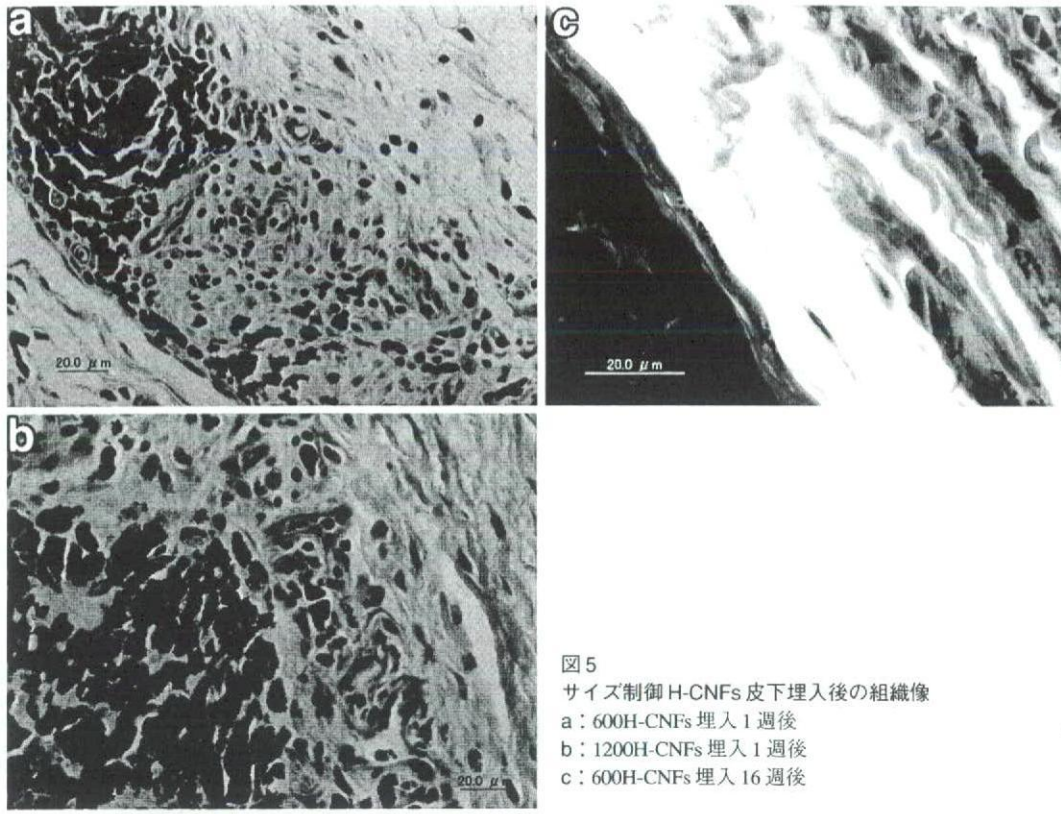

図5
サイズ制御H-CNFs皮下埋入後の組織像
a：600H-CNFs埋入1週後
b：1200H-CNFs埋入1週後
c：600H-CNFs埋入16週後

り，精製されたカーボンナノ物質としてハット積層型カーボンナノファイバー(hat stacked carbon nanofibers : H-CNFs)の供与を受け，予備実験的に埋入試験を行った．

H-CNFsの生体内挙動

1. H-CNFs

H-CNFsは，化学気相蒸着(CVD)によりNi触媒を用いて合成され，傘状のグラフェンシートが面間隔約0.34 nmで積層された形態をしている[20](図1)．

2. 埋入試験

長さ0.1～1 μm，直径30～100 nmのH-CNFsを，6週齢オス，ウィスターラットの胸部皮下組織に埋入した．1および4週で灌流固定後，周囲組織とともにH-CNFsを摘出し，浸漬固定を行った．通法に従いパラフィン包埋を行い，薄切後，ヘマトキシリン-エオジン染色を行い光学顕微鏡にて観察した．一部の試料については，Epon812に包埋後，約80 nmの超薄切片を作製し，酢酸ウラニルと硝酸鉛による重染色後，透過型電子顕微鏡(TEM)による観察を行った．

3. H-CNFsに対する反応

埋入1週後，H-CNFs集塊は，比較的薄い線維性結合組織の被膜で覆われており，H-CNFs粒子周囲には多数のマクロファージや異物巨細胞が認められた．これらの貪食系細胞の細胞質内にも，H-CNFsの小さな粒子が観察された(図2a, b)．4週後においてもH-CNFs粒子周囲には，間葉系の細胞や異物巨細胞が多数観察され，いわゆる肉芽腫性炎の状態を呈していたが，壊死や好中球の浸潤などの強い炎症反応は観察されなかった(図2c, d)．TEM観察において，1週後にマクロファージや異物巨細胞内に多数の貪食されたH-CNFs粒子が観察された．H-CNFsの多くは，互いに凝集し，膜に覆われてライソゾーム内に認められたが，一部に膜構造が観察されないものも認められた(図3)．これらの結果から，H-CNFsの起炎性は強くないこと，マクロファージに貪食されることが明らかとなった[15]．

細胞内でH-CNFsの長さの短縮や構造の変化を

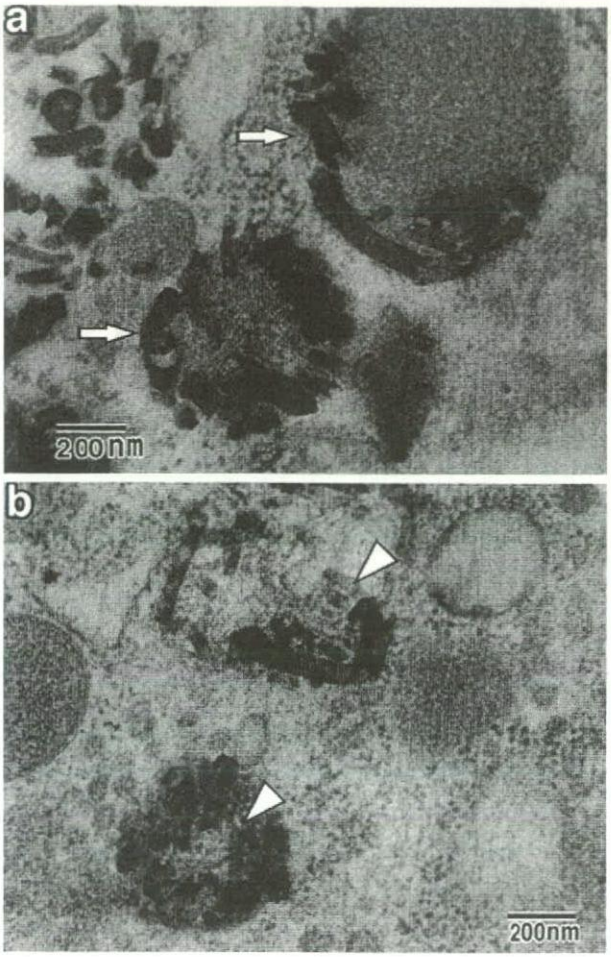

図6　600H-CNFs 皮下埋入後の TEM 像
a：埋入 1 週後．矢印：H-CNFs を取り込んだライソゾーム
b：埋入 16 週後．矢頭：短縮や半透明化した H-CNFs

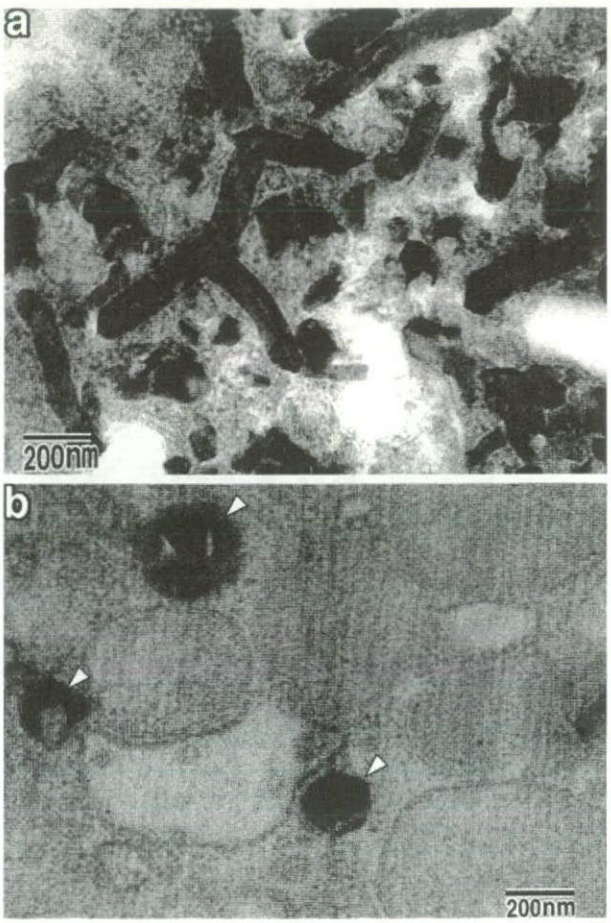

図7　1200H-CNFs 皮下埋入後の TEM 像
a：埋入 1 週後
b：埋入 16 週後．矢頭：短縮し，構造が変化したと推察される H-CNFs

示唆する所見も認められたが，埋入した H-CNFs の長さにばらつきがあることから，長さを制御するとともに，同じカーボンナノ物質でもグラフェンシートが継ぎ目のない状態でチューブ状を呈する構造がまったく異なる多層カーボンナノチューブ（MWCNTs）と比較するため，以下の研究を行った．

カーボンナノ物質のサイズと構造が細胞内挙動に及ぼす影響

1．試　料

精製しサイズを制御した H-CNFs と MWCNTs は，東北大学大学院環境科学研究科の田路研究室より供与を受けた．

（1）サイズ制御 H-CNFs

長さの制御は，濃硫酸（95%）：濃硝酸（60%）＝3：1（v/v%）の混合液に入れ，超音波照射により行った．洗浄，濾過後，さらにエタノール中で 1 時間超音波処理を行い，直径 2.0，1.2，および 0.4 μm の濾過膜で順に濾過し，平均長さ 590 nm と 1,160 nm の H-CNFs を得た（以下，600 H-CNFs および 1200 H-CNFs とする）（図 4a ～ c）．

（2）サイズ制御 MWCNTs

原材料として Nano Lab 社製の MWCNTs を用いた．

触媒を除去するため，塩酸および水酸化ナトリウムで洗浄後，95% 硫酸と 60% 硝酸を 3：1 で混合した溶液中で 5 時間超音波処理を行い，MWCNTs を精製した．得られた MWCNTs の長さを制御するため，エタノール中で 1 時間超音波処理し，ポリカー

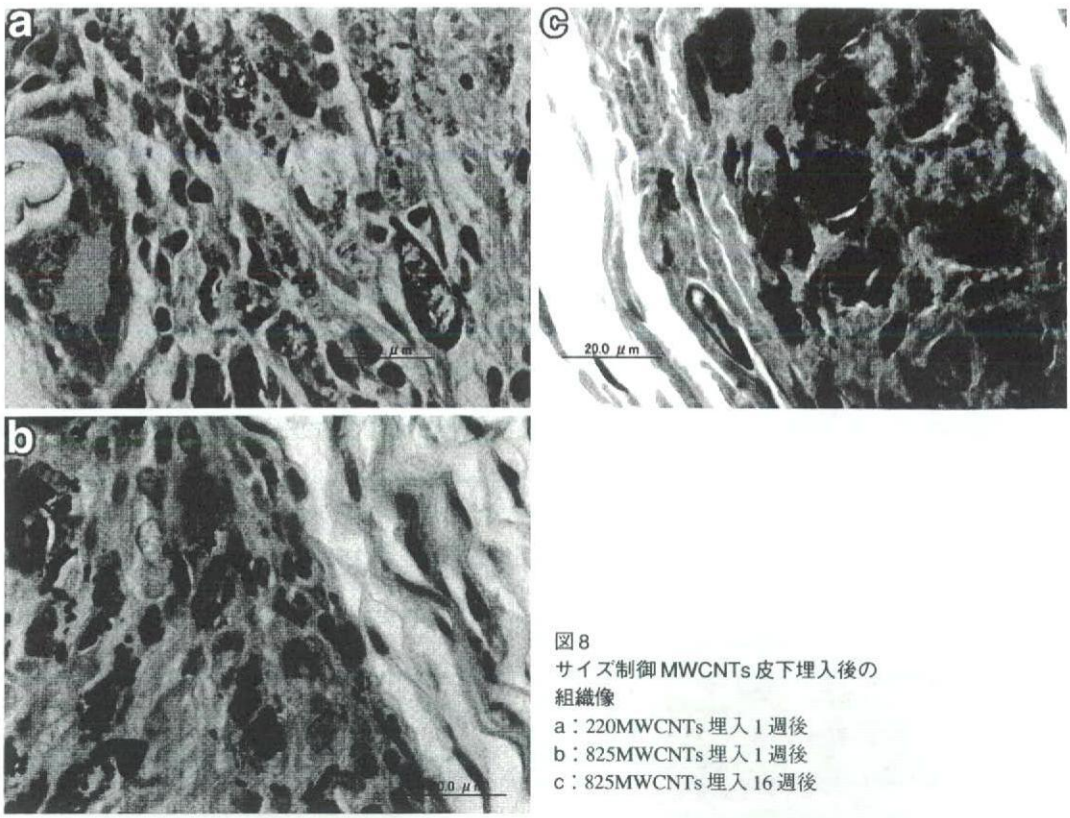

図8
サイズ制御MWCNTs皮下埋入後の組織像
a：220MWCNTs埋入1週後
b：825MWCNTs埋入1週後
c：825MWCNTs埋入16週後

ボネート製の直径2.0，1.2，0.8，および0.4 μmの濾過膜で順に濾過し，平均長さ220 nmおよび825 nmのMWCNTsを得た[18]（以下，220 MWCNTsおよび825 MWCNTsとする．精製およびサイズ制御の詳細については田路・佐藤論文を参照されたい）（図4d～f）．

2．カーボンナノ物質に対する反応

皮下組織への埋入試験は，長さ未制御のH-CNFsと同様に行ったが，観察期間は16週まで行った．

（1）H-CNFs

埋入1週後では，大きな塊状の600 H-CNFsは，線維性結合組織に被包されていたが，多くの600 H-CNFsはマクロファージや線維芽細胞に貪食されており，炎症は軽微であった（図5a）．16週後では，600 H-CNFsを貪食したマクロファージの集積が観察され，薄い線維性結合組織被膜に覆われていた．線維芽細胞内およびコラーゲン線維に沈着しているCNFsも観察された（図5c）．TEM観察では，1週後，多くの600 H-CNFsは細胞質内で円形に集合しており，ライソゾーム内にも600 H-CNFsが観察された（図6a）．16週後においては，ほとんどの600 H-CNFsは，ライソゾーム中に認められた．ライソゾーム中の600 H-CNFsには，長さの短縮，および半透明化などの結晶構造の変化を示唆する像も観察された（図6b）．

1200 H-CNFsは，1週後では，600 H-CNFsと同様にマクロファージや線維芽細胞に貪食されているものが多数認められたが，貪食されていないものが600 H-CNFsに比較し多く観察された．炎症は軽微であるが，600 H-CNFsに比較しやや強い傾向を示した（図5b）．16週後においては，600 H-CNFsとほぼ同様の所見を呈していた．TEM観察においては，1週では，細胞質内に1200-CNFsが多数観察されたが，ライソゾーム内には認められなかった（図7a）．16週では，細胞質内に円形に集合している1200 H-CNFsが多数認められ，一部のものはライソゾーム内に存在し，600 H-CNFsと同様に，短縮や結晶構造の変化を示唆する像が観察された（図7b）．

（2）MWCNTs

220 MWCNTsの多くは，埋入1週後において，マクロファージや線維芽細胞内に観察され，大きな集

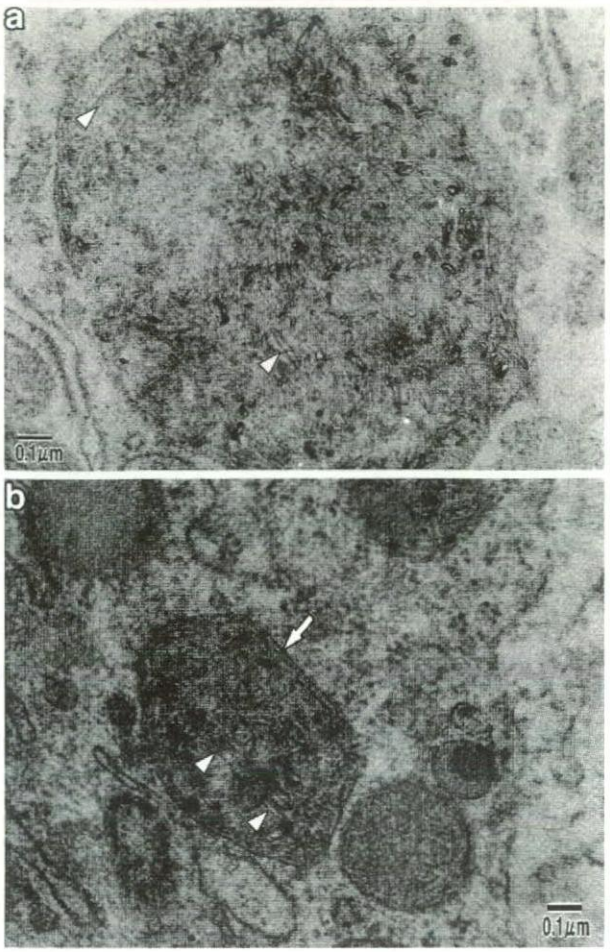

図9　220MWCNTs皮下組織埋入後のTEM像
a：埋入1週後．矢頭：ライソゾーム中のMWCNTs
b：埋入16週後．矢印：MWCNTsを取り込んだライソゾーム．矢頭：ライソゾーム中のMWCNTs

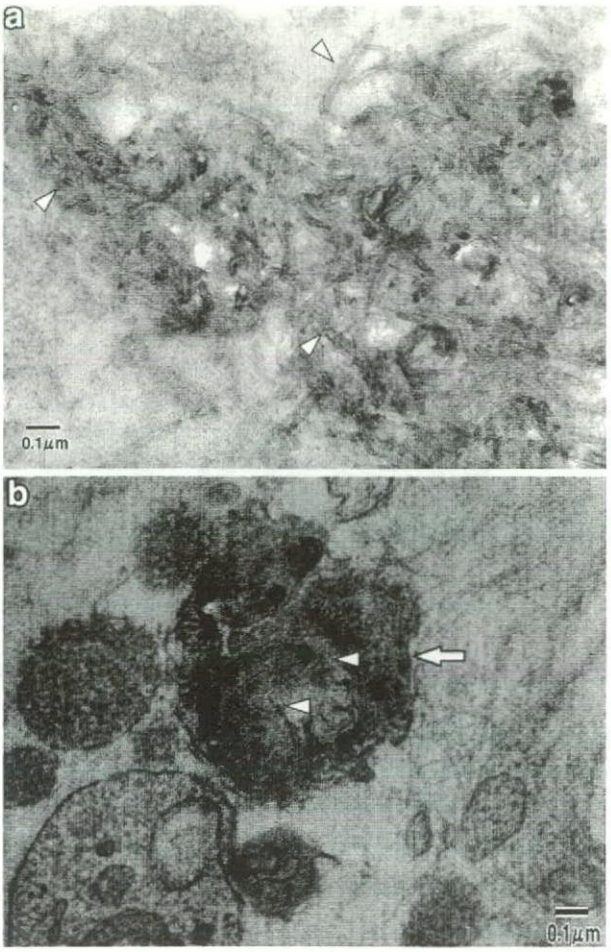

図10　825MWCNTs皮下組織埋入後のTEM像
a：埋入1週後．矢頭：細胞質中のMWCNTs
b：埋入16週後．矢印：MWCNTsを取り込んだライソゾーム．矢頭：MWCNTs

塊周囲には異物巨細胞が観察されたが，変性や壊死といった強い炎症反応は観察されなかった(図8a)．16週においては，220 MWCNTsはマクロファージやコラーゲン線維間の線維芽細胞中に観察された．比較的大きな集塊の周囲には異物巨細胞が観察されたが，強い炎症反応は認められなかった．TEM観察において，1週では，220 MWCNTsの多くは，マクロファージ中のライソゾーム内に観察された．220 MWCNTsは凝集しており，特有なチューブ状の形態には変化は認められなかった(図9a)．16週では，1および4週同様に220 MWCNTsは，マクロファージや線維芽細胞内のライソゾーム中に観察された．その多くは凝集しており，チューブ状の形態に変化は認められなかった(図9b)．

埋入1週後，825 MWCNTs周囲には肉芽組織が観察された．220 MWCNTsに比較すると炎症反応はやや強い傾向を示した．825 MWCNTsの一部は，マクロファージに貪食されていた(図8b)．埋入16週後では，825 MWCNTsの多くは，マクロファージや線維芽細胞内に観察されたが，一部の825 MWCNTsの集塊周囲に異物巨細胞が多数認められ，肉芽腫性炎を呈していた(図8c)．TEMにおいては，1週では，細胞間に多数の825 MWCNTsが観察されたが，マクロファージの細胞質内にも凝集したCNTsが認められ，膜構造で覆われていないものが多かった(図10a)．16週では，ライソゾームに存在する825 MWCNTsが多く認められるようになったが，そのチューブ状の構造に変化は観察されなかった(図10b)．

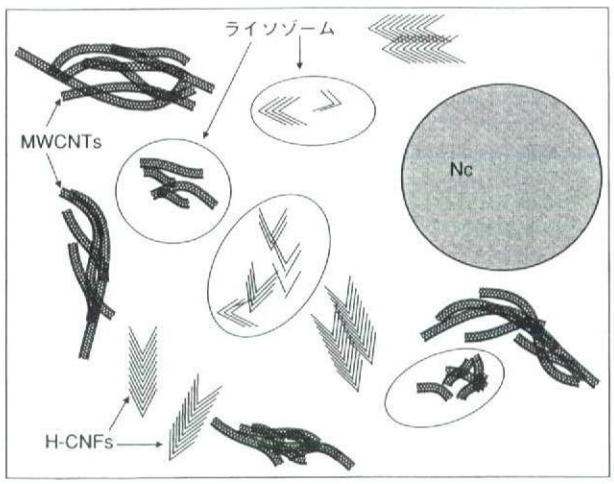

図11　カーボンナノ物質の細胞内での挙動の模式図
サイズの大きいもの，凝集の強いものはライソゾーム内には認められない．MWCNTsの構造は変化が認められないが，H-CNFsには短縮や結晶構造の変化が示唆される．このようにナノ物質のサイズや構造は細胞内挙動に影響する．

3．サイズと構造が起炎性と細胞内挙動に及ぼす影響

CNFsについては，観察した期間中，変性や壊死などの強い炎症反応は認められず，埋入初期に軽微な炎症が認められるにすぎなかった．長さが異なる2種を試料として用いたが，長い1200 H-CNFsの炎症反応のほうが，600 H-CNFsに比較しやや強い傾向を示した．この原因として，1200 H-CNFsのほうがマクロファージに貪食されにくいことが考えられる．これは，TEM所見からも裏付けられ，600 H-CNFsは，埋入1週においてライソゾーム中に認められるものがあり，多くのH-CNFsが，細胞質内において円形に集合していた．このことから，マクロファージ内でCNFsの処理が1週においてすでに進行していることが推察される．

1200 H-CNFsにおいても，16週後においては，ライソゾーム内に多数のH-CNFsが観察され，経時的にマクロファージ内で1200H-CNFsの処理が進んでいることが示唆された．これには，凝集しているH-CNFsの分散やH-CNFsの切断による短縮が関係するものと考えられる．

ライソゾーム中に観察されるH-CNFsは，いずれの長さのH-CNFsであっても，400 nm以下のものが多かった．短くなったものがライソゾームのなかに入りやすいのか，あるいはライソゾーム内でH-CNFsの切断と短縮が生じるのかは明らかではないが，H-CNFsは，マクロファージ内で処理される可能性が示唆された．

H-CNFsは，傘状のグラフェンシートが積層された構造をしており，1枚1枚のグラフェンシートはファンデルワールス力で結合しているため，切断には大きなエネルギーを要しない．また，グラフェンシートのエッジには水酸基があり，細胞内の酵素や蛋白と容易に結合することが可能であり，いわゆるデラミネーション[21]が起こりやすいこともH-CNFsの切断と短縮に関係するものと考えられる．また，興味深い所見として，埋入16週でライソゾーム内において一部に，H-CNFsの特有の構造である積層された傘状の構造に変化が認められた．これは，グラフェンシートの結晶構造の変化と考えられるが，詳細については今後さらなる研究が必要と考えられる．

細胞内でのH-CNFsの切断と短縮が示唆されたことは，DDSのキャリアとしての可能性を示すものであり，今後，生理活性物質と複合などの研究が期待される．

MWCNTsの起炎性は，H-CNFs同様に長いほうが起炎性は強く，埋入16週においても異物巨細胞が集積するいわゆる肉芽腫性炎が認められた．TEM所見からも，220 MWCNTsが1週後からライソゾーム内に認められるのに対し，825 MWCNTsでは，細胞間に存在するものが多く，細胞内においても細胞質内で凝集して存在しているものが多いことから，長いMWCNTsのほうが，マクロファージで処理されにくいことが示唆された．これは，Sato[18]が報告しているように，長いMWCNTsの凝集性のほうが強く，さらに825 MWCNTsは湾曲が強い形であり，凝集した状態から分離しにくいことなどに起因するものと推察された．16週においては，220 MWCNTsに比較するとその数は少ないが，825 MWCNTsにおいても一部のライソゾーム内にMWCNTsが観察された．

これらのことから，MWCNTsは細胞質，ライソゾーム内で蛋白や酵素の影響を受け凝集程度が弱くなったものと考えられた．また，H-CNFsと異なり，MWCNTsでは，切断，短縮や結晶構造の明らかな変化は認められず，チューブ状の構造が埋入16週においても維持されていた．これは，MWCNTsは炭素の六員環が連続している結晶構造をとるため，

機械的強度が強いだけでなく，化学的に安定であることも関係すると推察された．起炎性については，MWCNTsのほうがH-CNFsに比較し強い傾向を示したが，このような構造の差に基づく細胞の反応が関係している可能性が示唆された．

カーボンナノ物質に対する生体反応に関しては，冒頭で述べたように最近ようやく研究されるようになってきた．SWCNTsを気管内に強制曝露し，間質性の肉芽腫および壊死を報告したLam[13]は，CNTsの構造と物理化学的な性質によるものではないかと考察している．一方，Koyama[14]は，皮下にSWCNTs，MWCNTsなどのカーボンナノ物質を埋入し，アスベストに比較し起炎性が弱いことを報告している．しかし，これらの報告はいずれも光学顕微鏡レベルで観察されたものであり，ナノ物質の細胞内での挙動については，その大きさや構造を考慮するとTEMレベルでの検討も必要と思われる．また，埋入部位や濃度(量)などの条件も，生体反応に大きく関与するため，さらに，詳細かつ総合的な研究が必要であろう．

おわりに

これまでの研究で，同じカーボンナノ物質であっても，その構造や長さにより生体に対する反応および生体内での挙動が異なることが示唆された(図11)．現在，さらに長期埋入について検討を行っており，埋入1年後の結果が出つつある．今後，これらの結果を生体材料の開発に活かすとともに，さらにカーボンナノ物質の体内での動態などの安全性に関する研究を進めていく予定である．

本研究は，厚生科研費(H14-ナノ-021)，文部科学省科研費(16390549)によるものである．

文　献

1) Iijima S : Helical microtubules of graphitic carbon. Nature 1991, 354 : 56-58.
2) MurakamiT, Ajima K, Miyawaki J, Yudasaka M, Iijima S, Shiba K : Drug-loaded carbon nanohorns : Adsorption and release of dexamethasone *in vitro*. Mol Pharm 2004, 1 : 399-405.
3) Isobe H, Nakanishi W, Tomita N, Jinno S, Okayama H, Nakamura E : Nonviral gene delivery by tetraamino fullerene. Mol Pharm 2006, 3 : 124-134.
4) Fugetsu B, Satoh S, Shiba T, Mizutani T, Lin Y et al. : Caged multi-walled carbon nanotubes as the adsorbents for affinity-based elimination of Ionic dyes. Environmental Science & Technology 2004, 38 : 6890-6896.
5) Aoki N, Yokoyama A, Nodasaka Y, Akasaka T, Uo M et al. : Cell culture on a carbon nanotube scaffold. J of Biomed Nanotech 2005, 1 : 402-405.
6) Aoki N, Yokoyama A, Nodasaka Y, Akasaka T, Uo M et al. : Strikingly extended morphology of cells grown on carbon nanotubes. Chem Lett 2006, 35 : 508-509.
7) Schvedova AA, Castranova V, Kisin ER, Schwegler-Berry D, Murray AR et al. : Exposure to carbon nanotube material : assessment of nanotube cytotoxity using human keratinocyte cells. J Toxicol Environ Health A 2003, 21 : 1166-1170.
8) Monteiro-Riviere NA, Nemanich RJ, Inman AO, Wang YY, Riviere JE : Multi-walled carbon nanotubes interactions with human epidermal keratinocytes. Toxicol Lett 2005, 155 : 377-384.
9) Kirchner C, Liedl T, Kudera S, Pellegrino T, Javier AM et al. : Cytotoxicity of colloidal CdSe and CdSe/ZnS nanoparticles. Nano Lett 2005, 5 : 331-338.
10) Huczko A, Lange H : Carbon nanotubes : experimental evidence for a null risk of skin irritation and allergy. Fullerene Sci Technol 2001, 9 : 247-250.
11) Huczko A, Lange H, Calko E, Grubek-Jaworska H, Droszez P : Physiological testing of carbon nanotubes : are they asbestos-like? Fullerene Sci Technol 2001, 9 : 251-254.
12) Warheit DB, Laurence BR, Reed KL, Roach DH, Reynolds GAM, Webb TR : Comparative pulmonary toxicity assessment of single-wall carbon nanotubes in rats. Toxicol Sci 2004, 77 : 117-125.
13) Lam CW, James JT, McCluskey R, Hunter RL : Pulmonary toxicity of single-wall carbon nanotubes in mice 7 and 90 days after intratracheal instillation. Toxicol Sci 2004, 77 : 126-134.
14) Koyama S, Endo M, Kim YA, Hayashi T, Yanagisawa T et al. : Roll of systemic T-cells and histopathological aspects after subcutaneous implantation of various carbon nanotubes in mice. Carbon 2006, 44 : 1079-1092.
15) Yokoyama A, Sato Y, Nodasaka Y, Yamamoto S, Kawasaki T et al. : Biologocal behavior of hat-stacked carbon nanofibers in the subcutaneous tissue in rats. Nano Lett 2005, 5 : 157-161.
16) Uo M, Tamura K, Sato Y, Yokoyama A, Watari F et al. : The cytotoxicity of metal-encapsulating carbon nanocapsules. Small 2005, 1 : 816-819.
17) Sato Y, Shibata K, Kataoka H, Ogino S, Fugetsu B et al. : Strict preparation and evaluation of water-soluble hat-stacked carbon nanofibers for biomedical application and their high biocompatibility : influence of nanofiber-surface functional groups on cytotoxity. Molecular BioSystems 2005, 1 : 142-145.
18) Sato Y, Yokoyama A, Shibata K, Akimoto Y, Nodasaka Y et al. : Influence of length on biocompatibility of multi-walled carbon nanotubes by human acute monocytic leukemia cell line THP-1 *in vitro* and subcutaneous tissue of rats *in vivo*. Molecular BioSystems 2005, 1 : 176-182.
19) Yokoyama A, Sato Y, Nodasaka Y, Yamamoto S, Aoki N et al. : Tissue response to carbon nanosubstances : comparison between carbon nanotubes and hat-stacked carbon nanofibers by transmission electron microscopy. Extended Abstracts ISETS05 2005, 625-628.
20) Sato Y, Jeyadevan B, Tohji K, Tamura K, Akasaka T et al. : Water-soluble hat-stacked-type carbon nanofibers for biomedical applications. Abstract No 1625. 206th Meeting of ECS, 2004.
21) Liu Z, Ooi K, Kanoh H, Tang W, Tomida T : Swelling and delamination behaviors of birnessite-type manganese oxide by intercalation of tetraalkylammonium ions. Langmuir 2000, 16 : 4154-4164.

Strikingly Extended Morphology of Cells Grown on Carbon Nanotubes

Naofumi Aoki,*[1] Atsuro Yokoyama,[1] Yoshinobu Nodasaka,[1] Tsukasa Akasaka,[1] Motohiro Uo,[1] Yoshinori Sato,[2] Kazuyuki Tohji,[2] and Fumio Watari[1]

[1]*Graduate School of Dental Medicine, Hokkaido University, Kita 13, Nishi 7, Kita-ku, Sapporo 060-8586*

[2]*Graduate School of Environmental Studies, Tohoku University, Sendai 980-8576*

(Received February 7, 2006; CL-060164; E-mail: nao11@den.hokudai.ac.jp)

The morphology of cells cultured on carbon nanotube (CNTs) scaffolds was investigated using a confocal laser scanning microscope (CLSM) and a scanning electron microscope (SEM) and it was shown that the cells extended strikingly in all directions and numerous filopodia extended far from the cells.

Carbon nanotubes (CNTs) have attracted great interest since their discovery was reported by Iijima in 1991 because of their unique structure-dependent electrical and mechanical properties.[1] However, there have been very few studies on their biomedical application.[2,3] Some reports suggest the possible toxicity of CNTs.[4] In contrast, our recent studies employing in vitro and in vivo experiments showed their excellent properties as scaffolds for cell culture.[5,6] Cell morphology and proliferation have been investigated in in vitro studies, most of which were performed using nerve cells.[7] CNTs support nerve cell functions and growth, and our previous studies showed that the cells on CNTs grew well.[5] Thus, further investigation of interactions between CNTs and cells was deemed necessary to evaluate their biocompatibility and develop biological applications. There are only a few reports about the morphology of osteoblasts on CNTs.[8] The present study reports observations on the relationship between cells and CNTs and quantitative analysis of the morphology of osteoblasts grown on CNTs examined via scanning electron microscopy and confocal laser scanning microscopy, respectively.

CNTs 5–20 nm in diameter and 20–40 μm in length synthesized by chemical vapor deposition (NanoLab, Inc. MA, U.S.A.) were treated with hydrochloric acid to remove the metal catalyst. The purity was about 98 wt %.[9] CNTs (200 μg) were dispersed in 100 mL of deionized water by sonication for 3 min. CNT scaffolds were made by vacuum filtration of the dispersed CNT slurry onto porous polycarbonate membranes (PC; 47 mm diameter and 0.8 μm pore size, ADVANTEC, Japan). After drying for 3 h at 60 °C, CNTs were fixed on membranes, and coated and non-coated membranes were placed in polystyrene dishes 60 mm in diameter and sterilized under UV light for 24 h. Then, 1.0×10^5 human osteoblast-like cells (SaOS2 cells) were seeded onto each scaffold (PC and CNTs) and cultured in Dulbecco's modified Eagle's medium (DMEM; SIGMA) with 10% fetal bovine serum (FBS; Biowest) and 1% penicillin/streptomycin under standard cell culture conditions (at 37 °C in a humidified 5% CO_2/95% air environment) for 7 days. After cell culture for 7 days, the samples were washed with PBS to remove nonadherent cells on the scaffolds and fixed with a solution of 2% glutaraldehyde, and post-fixed in 1% osmium tetroxide. Then, the samples were dehydrated in graded series of alcohol (50, 70, 80, 90, 95, and 100%) and isoamyl acetate following critical-point drying. The cell morphology was observed and profiled using a confocal laser scanning microscope (CLSM; VK-9500, KEYENCE, Japan). A scanning electron microscope (SEM; S4000, Hitachi, Japan) was used for investigation of the peripheral parts of SaOS2 cells grown on CNTs.

Figure 1 shows the CLSM images demonstrating the morphology of SaOS2 cells cultured for 7 days on PC and CNTs. Note the difference of the scale bars. Cells on PC were elongated in one direction (Figure 1a), whereas there was excellent proliferation with extension of cells in all directions on CNTs (Figure 1b). The cells on CNTs were about 10 times larger than those on PC. Figure 2 shows a comparison of the cross-section profiles of from the different cultures. The length and the height of the cell were 12.13 and 6.83 μm on PC, and 113.14 and 4.35 μm on CNTs, respectively. The contact angle for the cell and substrate was much smaller on CNTs (4.4°) than that on PC (28.3°). The cells on CNTs were wider and flatter than those on PC.

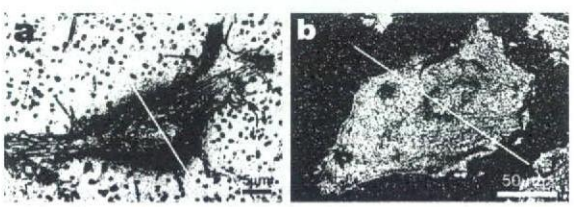

Figure 1. Cell morphology from culture on PC (a) and CNTs (b) observed by a confocal laser scanning microscope (CLSM). Note the difference of scale bars. Cells were fully developed on CNTs. The line show cross section referred to in Figure 2.

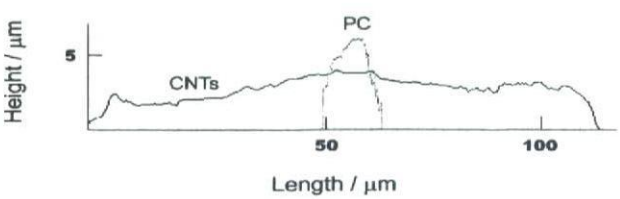

Figure 2. Comparison of cross-section profiles of cells shown in Figure 1.

Figure 3 shows the SEM images of the peripheral part of a cell on CNTs. Numerous filopodia 10–20 μm in length are extended and twisted on the CNT net with high density (Figure 3a). In the enlarged photograph (Figure 3b), the diameter of filopodia was comparable with CNTs and the apex of a filopodium is attached to the surface of CNTs.

In the present study, the difference of cell morphology on substrates with or without CNTs was investigated by SEM in vitro. Recently, toxicity of CNTs was reported;[4] however, our previous studies showed the number of cells on CNTs was larger

Copyright © 2006 The Chemical Society of Japan

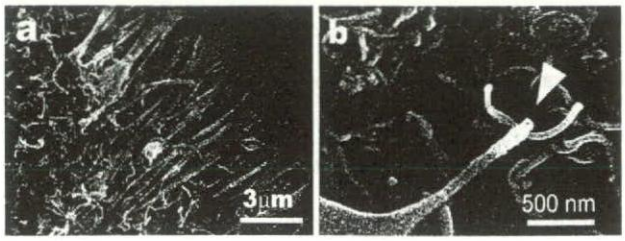

Figure 3. High-magnification SEM images of the peripheral part of SaOS2 cell grown on CNTs. a: Numerous fine filopodia extend toward CNT scaffolds. b: The apex of a filopodium attached on CNTs (arrowhead).

than the number of disseminated cells after 3 days, and cells on CNTs were more proliferated than those on PC.[5] The results of this study revealed that cells could adhere on CNTs and proliferate excellently.

The morphology of the cells with CNTs was markedly different from that of those without CNTs. Most of cells on CNTs were flat and spread in all directions. To evaluate the difference of cell morphology, quantitative analysis of cross-section profiles of cells was carried out using CLSM. The results showed that the length of cells on CNTs was as long as about 10 times that on PC, and the contact angle of cells on CNTs was less than one-sixth of that on PC. The cells on CNTs were clearly flatter. Additionally, the SEM images of cell periphery on CNTs revealed that numerous filopodia extended from cells toward the inside reticular CNTs. After treatment with trypsin to detach cells from CNTs, a few cells floated and showed a rounded-up shape. However, because of the mechanical binding of the filopodia extending from the cell bodies and twisted into CNT nets, most of the cells could not be detached from CNT scaffolds. The prominently flattered shape of cells, very small contact angle and growth of numerous filopodia suggested that CNTs had high affinity for adherence to human-derived osteoblastic cells. In contrast, few cells attached and grew on the graphite scaffolds. Although both CNTs and graphite consist of carbon, cell responses to them such as adhesion are quite different. Graphite is used as a material for heart valve prosthetics because it is nonthrombogenic. The difference of morphology between the fiber structure in CNTs and sheet structure in graphite would be one factor affecting their properties. The topology of the substrate affects the different aspects of cell behavior such as adhesion, proliferation, and morphology. Cell activity is influenced by microstructure and nanostructure. CNT scaffolds have a nanostructure, whereas PC membranes have a microstructure. The nanostructure, with its large surface area and high surface energy, may affect the morphology of cells on CNTs. In addition to surface topography, surface chemistry also plays a role in cell adhesion, proliferation, and morphology.[10] Various proteins such as extracellular matrix proteins and integrins may be related to cell adhesion. For example, the extracellular matrix of bone consists of collagenous proteins. In vitro, adsorption of proteins such as fibronection and vitronectin in serum onto materials may influence cellular responses. The CNTs surface was reported to be coated with various adsorbed molecules.[11] One possible explanation might be that the difference cellular response to CNTs and PC were caused by the difference of adsorption of protein. The excellent cell attachment and growth with numerous filopodia suggest that CNTs could be potential materials for various biomedical uses.

This work was supported by Health and Labour Science Research Grants in Research on Advanced Medical Technology in Nanomedicine Area from the Ministry of Health, Labour and Welfare of Japan and by a Grant (No. 16390549) from the Ministry of Education, Culture, Sports, Science and Technology of Japan.

References

1 S. Iijima, *Nature* **1991**, *354*, 56.
2 A. Bianco, K. Kostarelos, C. D. Partidos, M. Prato, *Chem. Commun.* **2005**, 571.
3 Y. Sato, K. Shibata, H. Kataoka, S. Ogino, F. Bunshi, A. Yokoyama, K. Tamura, T. Akasaka, M. Uo, K. Motomiya, B. Jeyadevan, R. Hatakeyama, F. Watari, K. Tohji, *Mol. Biosyst.* **2005**, *1*, 142.
4 K. F. Soto, A. Carrsco, T. G. Powell, L. E. Murrm, K. M. Garza, *Mater. Sci. Eng.*, in press.
5 N. Aoki, A. Yokoyama, Y. Nodasaka, T. Akasaka, M. Uo, Y. Sato, K. Tohji, F. Watari, *J. Biomed. Nanotechnol.* **2005**, *1*, 402.
6 A. Yokoyama, Y. Sato, Y. Nodasaka, S. Yamamoto, T. Kawasaki, M. Shindoh, T. Kohgo, T. Akasaka, M. Uo, F. Watari, K. Tohji, *Nano Lett.* **2005**, *5*, 157.
7 M. Mattson, R. C. Haddon, A. M. Rao, *J. Mol. Neurosci.* **2000**, *14*, 175.
8 K. L. Elias, R. L. Price, T. J. Webster, *Biomaterials* **2002**, *23*, 3279.
9 Y. Sato, A. Yokoyama, K. Shibata, Y. Akimoto, S. Ogino, Y. Nodasaka, T. Kohgo, K. Tamura, T. Akasaka, M. Uo, K. Motomiya, B. Jeyadevan, M. Ishiguro, R. Hatakeyama, F. Watari, K. Tohji, *Mol. Biosyst.* **2005**, *1*, 176.
10 K. Anselme, *Biomaterials* **2000**, *21*, 667.
11 T. Akasaka, F. Watari, *Chem. Lett.* **2005**, *34*, 826.

Published on the web (Advance View) April 8, 2006; DOI: 10.1246/cl.2006.508

Dental Materials Journal 26(2): 178–185, 2007

Carbon Nanotubes as Scaffolds for Cell Culture and Effect on Cellular Functions

Naofumi AOKI, Tsukasa AKASAKA, Fumio WATARI and Atsuro YOKOYAMA
Graduate School of Dental Medicine, Hokkaido University, Kita 13, Nishi 7, Kita-ku, Sapporo 060-8586, Japan
Corresponding author, Naofumi Aoki; E-mail: nao11@den.hokudai.ac.jp

Received October 11, 2006 /Accepted November 8, 2006

To investigate the dependence of biocompatibility of carbon materials on crystal structure with the aim of developing biomedical applications, single-(SW) and multi-walled (MW) carbon nanotubes (CNTs) were employed as scaffolds for cell culture and compared with graphite (GP). SaOS2 cells were used to investigate the properties and response of osteoblast-like cells. Polycarbonate membranes (PC) coated with CNTs by vacuum filtration formed a meshwork nanostructure. Cells grown on CNTs greatly extended in all directions. In terms of cell proliferation, alkaline phosphatase (ALP) activity, and protein adsorption on the substrates, CNTs showed better results than PC and GP. SW showed the best cell proliferation and total ALP. These favorable results might be attributed to the structure of CNTs and the affinity of CNTs toward proteins, thereby suggesting that CNTs could be potential scaffold materials for cell culture.

Keywords: Carbon nanotubes, Scaffold, Osteoblast

INTRODUCTION

In the imminent ageing society of the 21st century, nanotechnology[1,2] is a core technology to promoting health and improving QOL (quality of life) by enabling new health care technologies. In this connection, nanomaterials have been widely investigated for potential application in the medical field—ranging from making improved diagnostic methods to drug delivery systems, and from tissue regeneration to artificial prostheses[3,4]. In particular, carbon nanotubes (CNTs)—one of the most representative nanomaterials—were first reported by Iijima in 1991[5]. CNTs consist of carbon atoms and have unique electronic, catalytic, chemical, and mechanical properties[6]. Although CNTs have been widely studied, most of the studies focused on the physical, electrical, and chemical fields, with very few on biomedical applications[7-9].

Of late, there were reports on possible toxicity of CNTs[10-13], arising from their fibrous structure which resembles that of asbestos fibers causing lung cancer. Logically then, their safety as a biomaterial has been a matter of grave concern. Against this background, our previous *in vivo* and *in vitro* studies on nanocarbon materials investigated their possible use as a biomaterial. Yokoyama *et al.*[14] reported that hat-stacked carbon nanofibers did not cause a severe inflammatory response, and Wang *et al.*[15] reported that sintered bulk carbon nanotube materials exhibited sufficient biocompatibility. Moreover, Aoki *et al.*[16,17] reported on cell proliferation on multi-walled CNTs. Nonetheless, further investigations on cell functions such as enzymatic activity were deemed necessary to evaluate their biocompatibility for the development of biological applications.

The last decade has seen a dramatic development in biomedical technology, especially bone regeneration in tissue engineering. Scaffolds play a key role in most tissue engineering strategies[18,19]. In particular for bone bioengineering, one of the most important steps is to create scaffold materials that have the capacity to sustain bone cell growth and proliferation, as well as increment or replace bone tissue[20]. To date, scaffolds constructed with various materials such as porous polymers and ceramics have been reported[21,22]. Then recently, there have been several reports on the application of CNTs for scaffolds due in part to their unique mechanical, physical, and chemical properties[16,17,20,23]. For example, Mattson *et al.*[24] reported that CNTs coated with bioactive molecules were used as substrates for nerve cell growth. Webster *et al.*[25] reported that carbon nanofibers increased osteoblast functions. Similarly, MacDonald *et al.*[26] demonstrated that collagen-CNT composite materials could be used as scaffolds in tissue engineering.

CNTs come in two principal types: multi-walled (MW) and single-walled (SW). Due to their different crystal structures, these two types of CNTs show different electronic, catalytic, physical, and chemical properties. CNTs are also compared with graphite (GP). Both are isomorphs of pure carbon, composed of the same graphene sheet structure—where CNTs have the cylindrical structure, while GP have the layered sheet structure. However, there is scarce information about cellular response to the different crystal structures. The aim of the present study,

therefore, was to investigate the biological responses of cell proliferation and function on CNT scaffolds and their dependence on the crystal structures of MW and SW using osteoblast-like cells (SaOS2). These osteoblast cell responses were then compared with those of GP.

MATERIALS AND METHODS

Materials

MW carbon nanotubes of 5–20 nm in diameter and 20–40 μm in length synthesized by the chemical vapor deposition technique with purity of 98.17% (NanoLab Inc., MA, USA) were treated with hydrochloric acid to remove metal catalysts[27]. SW of 1.3–1.5 nm in diameter and 2–3 μm in length synthesized by arc discharge with purity of 99.56% (NanoLab Inc., MA, USA) were also treated in the same way. The GP particles used in this study were 4.5 μm in diameter.

Fabrication of scaffolds

CNTs and GP (200 μg) were dispersed in 100 mL of deionized water by sonication for 15 minutes. Then, scaffolds were made by vacuum filtration of the dispersed CNTs and GP slurry onto a porous polycarbonate membrane of 47 mm diameter and 0.8 μm pore size (PC; Adavantec, Japan). After drying for 3 hours at 60℃, CNTs and GP were fixed on the membranes. Scaffolds were sterilized by ultraviolet radiation for 24 hours prior to experiments with cells. The morphology of scaffolds was examined by scanning electron microscopy (SEM; S–4000, Hitachi, Japan).

Evaluation of protein adsorption on scaffolds

For the evaluation of protein adsorption on scaffolds, each scaffold was immersed in 2 mL of Dulbecco's modified Eagle's medium (DMEM; SIGMA) with 10% fetal bovine serum (FBS; Biowest) used for cell culture. After 24 hours incubation at 37℃, the substrates were washed three times with PBS, sonicated for 15 minutes, and centrifuged (12000 rpm) for 3 minutes to separate proteins from the substrates. Aliquots of the removed solution were analyzed by the BCA method.

Cell culture

The scaffolds were placed in polystyrene dishes of 60 mm diameter. Then, 1.0×10^5 human osteoblast-like cells (SaOS2) were seeded onto each scaffold and cultured in Dulbecco's modified Eagle's medium (DMEM; SIGMA) with 10% fetal bovine serum (FBS; Biowest) and 1% penicillin-streptomycin under the standard cell culture conditions (at 37℃ in a humidified 5% CO_2/95% air environment) for 3 and 7 days. The medium was changed every other day.

Cell proliferation

For the evaluation of cell proliferation, cells were cultured for 3 and 7 days on the substrates. Cell proliferation was evaluated by counting the number of cells attached to each scaffold in SEM micrographs. For SEM observation, at the end of each prescribed time period, the substrates were rinsed with PBS to remove non-adherent cells on the membranes, fixed in a solution of 2% glutaraldehyde, and post-fixed in a 1% osmium tetroxide solution. The samples were then dehydrated in a series of solutions with increasing ethanol concentrations, followed by critical-point drying at 40℃. All the experiments were repeated four times. The numbers of cells were counted in 10 random fields per scaffold and averaged. Objects less than 10 μm in diameter were not included in the attached cell count.

Alkaline phosphatase activity

Alkaline phosphatase (ALP) activity was measured with LabAssay ALP (Wako, Japan). The culture medium was removed and the dishes were rinsed three times with PBS. Cells on the substrates were scraped, incubated with 1000 μl of CelLytic-M (Sigma) for 15 minutes on a shaker, and centrifuged (500 g) for 15 minutes. Samples of 20 μl were added to 100 μl of *p*-nitrophenol phosphatase in a carbonate buffer and incubated for 15 minutes at 37℃. After 80 μl of NaOH was added, absorbance was measured at 405 nm (Benchmark, Bio-Rad, USA) and enzyme activity was determined from the calibration curve of *p*-nitrophenol standard. ALP activity was normalized by total protein content measured by a BCA protein assay kit (Pierce, USA) and expressed as μmol *p*-nitrophenol/mg protein.

Statistical analysis

All the experiments on protein adsorption, cell proliferation, and ALP activity were repeated four times. Statistical significance between groups was calculated using the Mann-Whitney U test with Bonferroni correction under the condition of $p<0.05$.

RESULTS

SEM images of scaffolds

Fig. 1 shows the SEM images of scaffolds. GP (b) on PC (a) was a particle of about 5 μm in size. There were little differences in the fibrous morphology between MW (c) and SW (d) on PC. Both CNTs formed a densely packed meshwork nanostructure (Figs. 1(c) and (d)). The diameter of SW resembled that of MW, coupled with a formation of bundles.

Cell morphology

Fig. 2 shows the SEM images of the morphology of SaOS2 cells cultured for 3 and 7 days on each

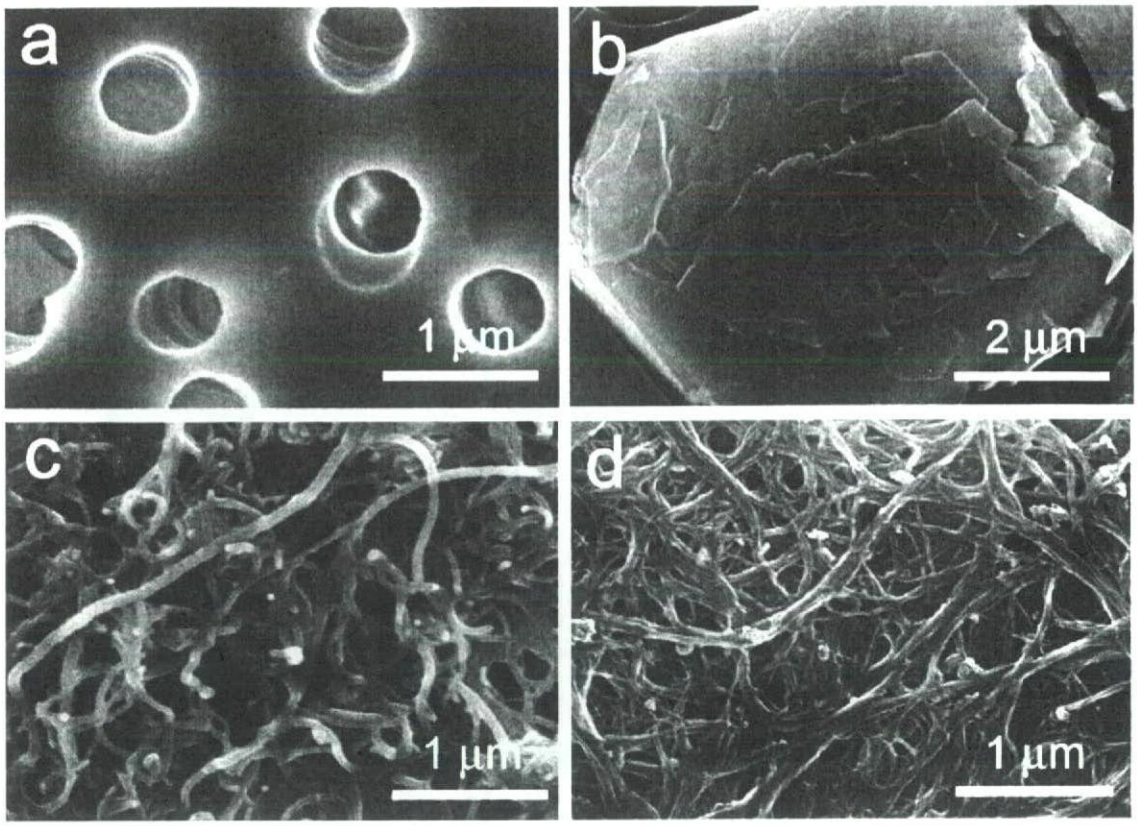

Fig. 1 SEM images of scaffolds: PC (a), GP (b), MW (c), and SW (d).

scaffold. Except on GP, cells proliferated and spread with incubation time. The cells on SW grew nearly to confluence after 7 days. The morphology of the cells on CNTs was markedly different from that on non-CNT scaffolds. Most of the cells on PC were elongated in one direction (Fig. 2(a)) and those on GP were round (Fig. 2(b)), whereas those on CNTs extended in all directions and proliferated well (Figs. 2(c) and (d)). As for comparison between MW and SW, it could be seen that the cells exhibited similar morphology.

Amount of adsorbed proteins on scaffolds

Fig. 3 shows the amounts of adsorbed proteins on the scaffolds immersed in cell culture medium after 24 hours. Proteins in medium were adsorbed to a certain extent depending on the substrate. CNT scaffolds showed higher values than PC and GP. Between CNTs, adsorption on SW was about twice as high as that on MW.

Cell proliferation

Fig. 4 shows the number of proliferated SaOS2 cells after 3 and 7 days. Few cells were attached and proliferated on GP. The number of cells attached to the CNTs was significantly larger than on PC and GP for all the proliferation periods ($p<0.05$). Between CNTs, the number of cells on SW was similar to that on MW at 3 days, but significantly increased to 2.7 times that of MW at 7 days ($p<0.05$).

Alkaline phosphatase activity

Fig. 5 shows the ALP activity (expressed as *p*-nitrophenol mmol/L) of the cells on each substrate at 3 and 7 days. The ALP activity increased with time for all the substrates. CNTs showed higher activity than PC and GP and increased from 3 to 7 days. SW showed the highest increase of ALP activity at 7 days.

Fig. 6 shows the ALP activity normalized by total protein content at 3 and 7 days. Except for GP, the ALP activity increased with time for all the substrates. Nonetheless, CNTs showed higher activity than PC at 3 and 7 days. For scaffolds made of carbon, they were similar at 3 days but SW was the highest at 7 days.

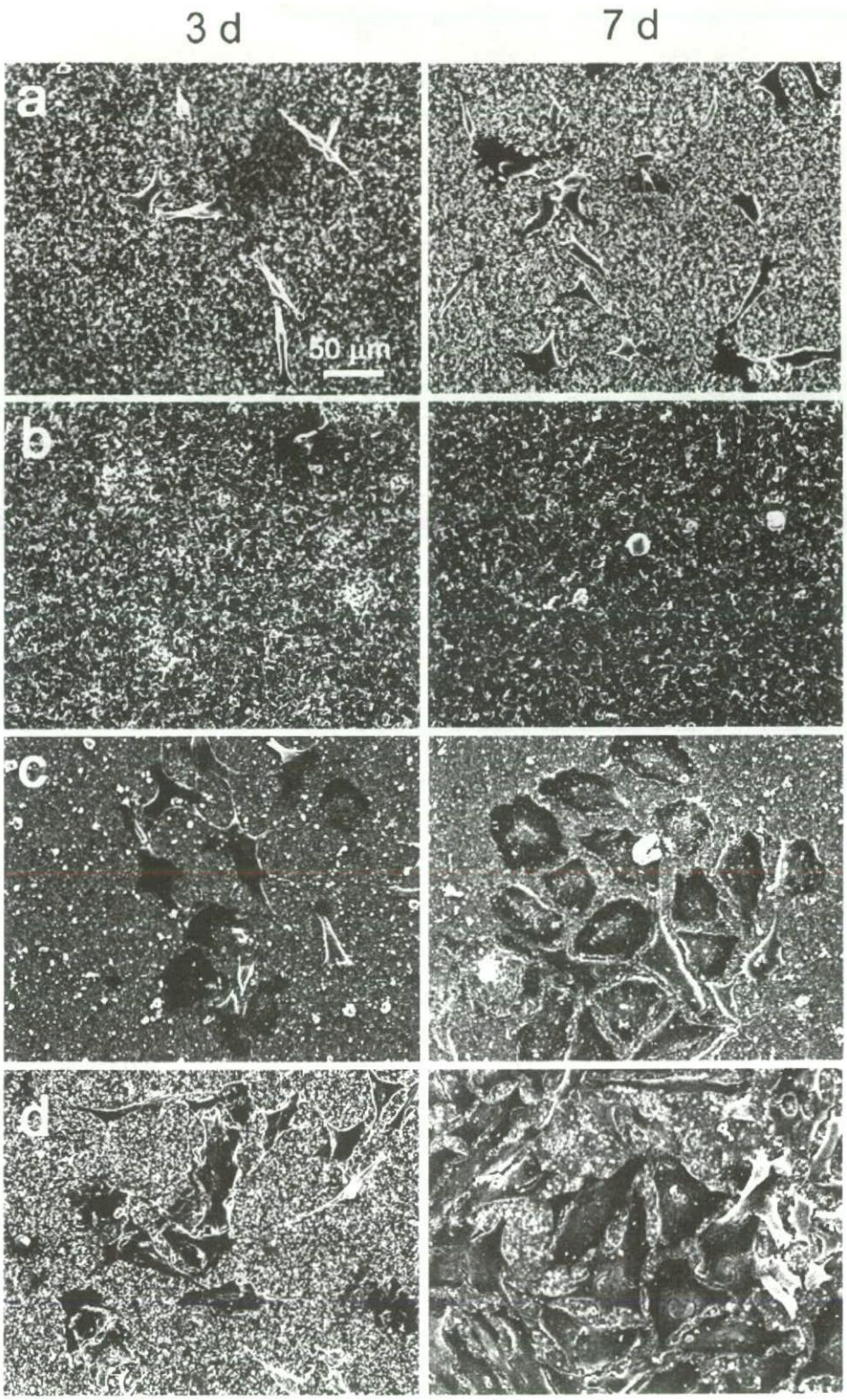

Fig. 2 SEM images of cells cultured for 3 days (left) and 7 days (right) on: PC (a), GP (b), MW (c), and SW (d).

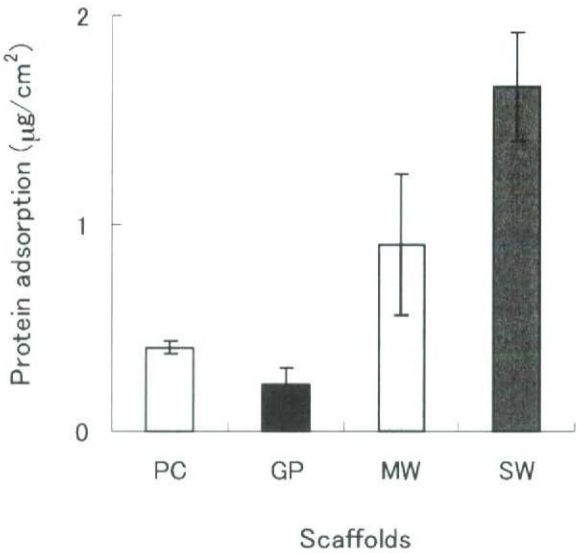

Fig. 3 Amounts of adsorbed proteins on the scaffolds immersed in cell culture medium after 24 h.

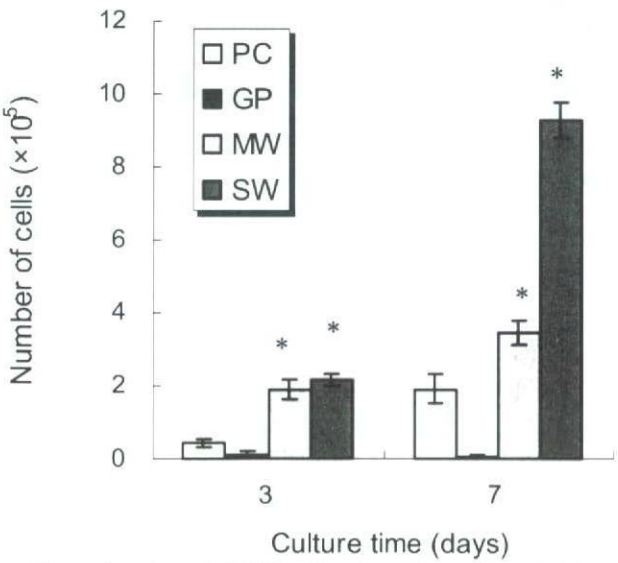

Fig. 4 Number of SaOS2 cells cultured on the scaffolds at 3 and 7 days, where '*' indicates significant difference at $p<0.05$ upon comparison between respective substrates at 3 and 7 days.

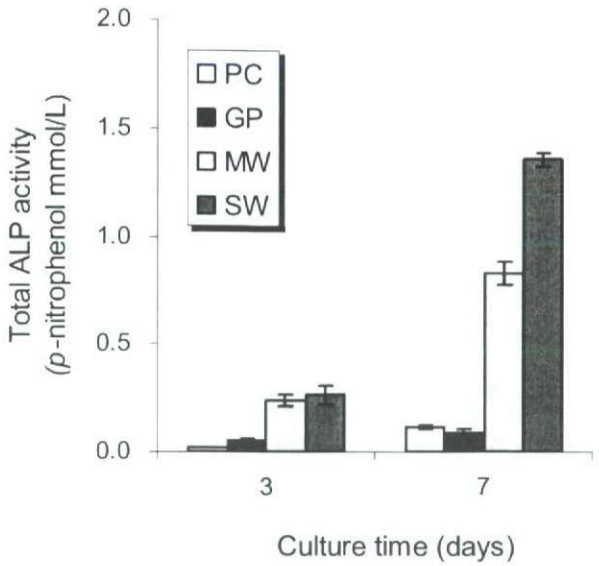

Fig. 5 Total ALP activity of cells cultured on the scaffolds at 3 and 7 days.

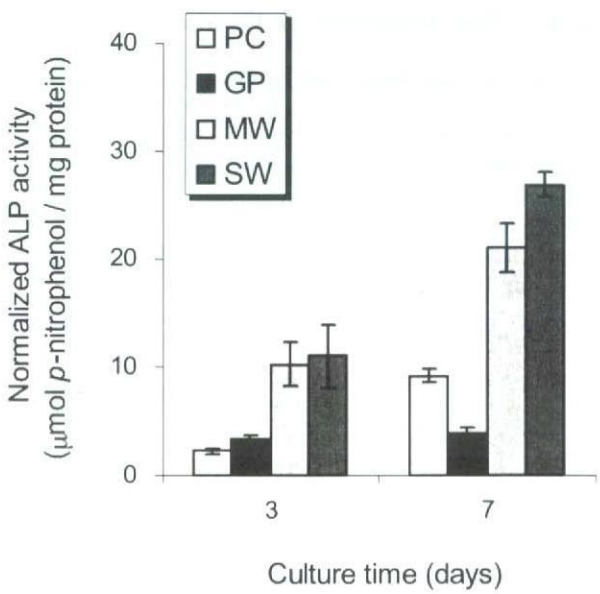

Fig. 6 ALP activity normalized by total protein content in a μmol p-nitrophenol/mg protein unit.

DISCUSSION

Cell morphology

The present *in vitro* study demonstrated that cell morphology was affected by the scaffolds. SEM images showed that CNT scaffolds presented a fibrous nanostructure, while PC and GP scaffolds had microporous or microparticle structure, respectively. Scaffolds should have properties favorable for cell attachment and growth[21]. Cells that develop in a flat form with a small contact angle have stronger binding and affinity to the scaffold than those that are round with a large contact angle[17]. The present study showed that the cells on CNTs extended in all directions, whereas cells on PC and GP had a spindle or round shape. Our previous studies showed that cells on MW extended in all directions[16,17]. Similarly, cells on SW showed strikingly extended morphology with a diameter of approximately 100 μm. The morphology of osteoblasts that spread flatly on CNTs resembled the case of titanium which has good biocompatibility[28]. Thus, it could be said that CNTs